Contribution from the Department of Chemistry,
The University of Alberta, Edmonton, Alberta, Canada T6G 2G2

Structure of $[RhCl(H)((C_6H_5)_2PCH_2P(C_6H_5)_2)_2][B(C_6H_5)_4]$: A Rhodium(III) Hydrido Complex Containing Chelating Bis(diphenylphosphino)methane Ligands

MARTIN COWIE* and STEPHEN K. DWIGHT

Received November 16, 1978

The reaction of the anionic species $[RhCl_2(CO)_2]^-$ with bis(diphenylphosphino)methane (DPM) yields two different products depending on the DPM:Rh molar ratio. An X-ray crystallographic study of the product, obtained with a 2:1 molar ratio of DPM:Rh, proved it to be $[RhCl(H)((C_6H_5)_2PCH_2P(C_6H_5)_2)_2][B(C_6H_5)_4]$, a monomeric species containing chelating DPM ligands and mutually trans chloro and hydrido ligands. The complex crystallizes in the space group C_{2h}^5-$P2_1/c$ in a cell of dimensions $a = 19.477$ (2) Å, $b = 15.266$ (2) Å, $c = 22.282$ (2) Å, and $\beta = 106.85$ (1)° with $Z = 4$. On the basis of 6832 unique reflections the structure was refined by full-matrix, least-squares techniques to agreement indices of $R = 0.064$ and $R_w = 0.084$. Some relevant metric parameters are Rh–P(av) = 2.329 (3) Å, Rh–Cl = 2.465 (2) Å, Rh–H(1) = 1.51 (7) Å, P(1)–Rh–P(2) = 72.47 (6)°, P(3)–Rh–P(4) = 72.43 (7)°, and H(1)–Rh–Cl = 172 (3)°. The $\overline{\text{Rh–P–C–P}}$ chelate frames are not planar, having the methylene groups approximately 0.338 (7) Å out of their respective P–Rh–P planes.

Introduction

As part of our continuing investigations into the chemistry of binuclear rhodium(I) complexes,[1-4] we reacted the binuclear "A-frame" complex $[Rh_2(CO)_2(\mu\text{-}Cl)(DPM)_2][BPh_4]$ (**1**) (Ph = C_6H_5, DPM = $Ph_2PCH_2PPh_2$) with SO_2 in order to ascertain the site of attack and mode of coordination of the SO_2 molecule.[3,4] Attempts to recrystallize the initial SO_2 adduct, complex **2**, under a prolonged stream of SO_2, however, resulted in a disproportionation reaction as shown.

$$\underset{\mathbf{1}}{[Rh_2(CO)_2(\mu\text{-}Cl)(DPM)_2][BPh_4]} \xrightarrow{SO_2}$$

$$\underset{\mathbf{2}}{[Rh_2(CO)_2(\mu\text{-}SO_2)(\mu\text{-}Cl)(DPM)_2][BPh_4]} \xrightarrow[SO_2]{\text{prolonged}}$$

$$\underset{\mathbf{3}}{[Rh_2Cl_2(\mu\text{-}SO_2)(DPM)_2]} + \underset{\mathbf{4}}{[?]}$$

The first disproportionation product, complex **3**, which precipitated as red-orange crystals, was identified by spectroscopic techniques and by a single-crystal X-ray diffraction study.[3,4] The remaining yellow solution containing the other disproportionation product (or products), **4**, then became the subject of our investigations.

A subsequent attempt to repeat the above disproportionation reaction, under seemingly identical conditions, resulted in the precipitation of yellow prisms during the reaction of **1** with SO_2. Although, on the basis of a comparison of ^{31}P NMR spectra, it was evident that this yellow complex was not one of the disproportionation products, infrared and ^{31}P and ^1H NMR spectra indicated that it was an unexpected hydridorhodium complex. An X-ray structural investigation was therefore undertaken to establish unambiguously the identity of this hydrido species and a chemical investigation was carried out to establish the relationship of this species to the above reaction scheme.

Experimental Section

Infrared spectra were recorded on a Nicolet 7199 F.T. interferometer by using Nujol mulls on KBr plates, and ^{31}P and ^1H NMR spectra were recorded by using a Digilab pulse Fourier transform equipped Varian HA-100. Elemental analyses were done within the department. All reactions were carried out under inert or reactant gas atmospheres by using standard Schlenk techniques, and all solvents were degassed prior to use. Hydrated Rh(III) chloride was purchased from Research Organic/Inorganic Chemicals and bis(diphenylphosphino)methane was purchased from Strem Chemicals.

Preliminary Isolation of $[RhCl(H)(DPM)_2][BPh_4]$. A sample of 0.20 g of "$[Rh_2(\mu\text{-}Cl)(CO)_2(DPM)_2][BPh_4]$" (see ref 1 for preparation) was dissolved in a minimum volume of acetone. Sulfur dioxide was then passed through the flask for approximately 20 min and the flask sealed under an atmosphere of SO_2. Yellow crystals of $[RhCl(H)(DPM)_2][BPh_4]$, suitable for single-crystal X-ray diffraction study, began forming after 2 h. Anal. Calcd for $C_{74}H_{65}BClP_4Rh$: C, 72.4; H, 5.3; Cl, 2.9. Found: C, 72.7; H, 5.3; Cl,[5] 0.0. IR: ν(Rh–H) 2080 cm^{-1}. ^1H NMR (−50 to +30 °C): $\tau = 21.9$ (doublet of quintets, $J_{Rh-H} = 17.5$ Hz, $J_{P-H} = 13.0$ Hz), $\tau = 5.05$ and $\tau = 5.65$ (each is a doublet of quintets), $\tau \simeq 2.8$ (multiplet). $^{31}P\{^1H\}$ NMR: $\delta = -15.8$ (downfield from H_3PO_4 is positive, $J_{Rh-P} = 83$ Hz).

X-ray Data Collection. A crystal of the title compound of approximate dimensions 0.25 × 0.40 × 0.37 mm was mounted in a sealed capillary. Preliminary film data showed that the crystal belonged to the monoclinic system with extinctions ($h0l$, l odd; $0k0$, k odd) characteristic of the centrosymmetric space group $P2_1/c$. Accurate cell parameters were obtained by a least-squares analysis of 12 carefully centered reflections chosen from diverse regions of reciprocal space ($60° < 2\theta < 70°$, Cu Kα radiation) and obtained by using a narrow X-ray source. See Table I for pertinent crystal data and the details of data collection. The width at half-height of several strong, low-angle reflections (ω-scan, open counter) lay in the range 0.15–0.17°.

Data were collected by the θ–2θ scan method on a Picker four-circle automated diffractometer equipped with a scintillation counter and pulse height analyzer, tuned to accept 90% of the Cu Kα peak. Background counts were measured at both ends of the scan range with the counter and crystal stationary. The intensities of three standards were measured every 100 reflections. In addition four other standard reflections were measured three times a day. All standards decomposed by approximately 8% over the duration of the data collection. The observed intensities were corrected for this apparent decomposition.

The intensities of 9809 unique reflections ($3° \leq 2\theta \leq 120°$) were measured by using Cu Kα radiation. Data were processed in the usual manner by using a value of 0.05 for p.[6] A total of 6833 reflections had $F_o^2 \geq 3\sigma(F_o^2)$ and were used in subsequent calculations. Absorption corrections were applied to the data by using Gaussian integration.[7]

Structure Solution and Refinement. The structure was solved by using a sharpened Patterson synthesis to locate the Rh atom. Subsequent refinements and difference Fourier syntheses led to the location of all remaining atoms. Atomic scattering factors were taken from Cromer and Waber's tabulation[8] for all atoms except hydrogen for which the values of Stewart et al.[9] were used. Anomalous dispersion terms[10] for Rh, P, and Cl were included in F_c. Ten of the phenyl groups were refined as rigid groups having D_{6h} symmetry and C–C distances of 1.392 Å; the carbon atoms in these groups were given independent, isotropic thermal parameters. The two remaining phenyl groups, because of their abnormally high thermal parameters (B's up to 16 Å^2), were refined as independent atoms with anisotropic thermal parameters. The hydrido ligand was located in a difference Fourier synthesis and refined with an isotropic thermal parameter. The remaining hydrogen atoms were included as fixed contributions and not refined. Their idealized positions were calculated from the

0020-1669/79/1318-1209$01.00/0

Table I. Summary of Crystal Data and Intensity Collection

compd	$[RhCl(H)(DPM)_2][BPh_4]$
formula	$C_{74}H_{65}BClP_4Rh$
formula wt	1227.41
a	19.477 (2) Å
b	15.266 (2) Å
c	22.282 (2) Å
β	106.85 (1)°
V	6340.6 $Å^3$
Z	4
density	1.285 g cm^{-3} (calcd) 1.283 (5) g cm^{-3} (exptl by flotation)
space group	C_{2h}^5-$P2_1/c$
crystal dimens	0.250 × 0.405 × 0.371 mm
crystal vol	0.0413 mm^3
crystal shape	monoclinic prism with faces of the form {100} and {012}
temp	20 °C
radiation	Cu Kα (λ 1.540 562 Å) filtered with 0.5 mil thick nickel foil
μ	38.976 cm^{-1}
range in absorption correction factors (applied to F_o)	0.570–0.688
receiving aperture	4 × 4 mm, 30 cm from crystal
takeoff angle	3.3°
scan speed	2° in 2*θ*/min
scan range	0.95° below $Kα_1$ to 0.95° above $Kα_2$
background counting	10 s ($2\theta \leq 65°$); 20 s ($65° < 2\theta \leq 95°$); 40 s ($95° < 2\theta \leq 120°$)
2*θ* limits	3.0–120.0°
final no. of variables	314
unique data used ($F_o^2 \geq 3\sigma(F_o^2)$)	6832
error in observn of unit weight	2.190 e
R	0.064
R_w	0.084

geometries about the attached carbon atom by using C–H distances of 0.95 Å. Isotropic thermal parameters (of 1 $Å^2$ greater than their attached carbon atom) were given to these hydrogen atoms. All other nongroup atoms were refined individually with anisotropic thermal parameters. The final model with 314 parameters varied converged to $R = 0.064$ and $R_w = 0.084$.[11] In the final difference Fourier map all of the highest 20 residuals were in the vicinity of the phenyl groups (0.40–0.69 e/$Å^3$). A typical carbon atom on earlier syntheses had an electron density of about 3.8 e/$Å^3$. It seems that anisotropic refinement of the other phenyl carbon atoms would have been more suitable on the basis of the thermal parameters of some of these group atoms and the residuals about the phenyl groups. However, this was not attempted owing to the very high cost and the fact that the previous refinements of the two phenyl groups as individual atoms with anisotropic thermal parameters resulted in no significant changes in the parameters of interest.

The final positional and thermal parameters of the individually refined atoms and the group atoms are given in Tables II and III. The idealized hydrogen positions and their thermal parameters, the root-mean-square amplitudes of vibration of the individual nonhydrogen atoms, and a listing of observed and calculated structure amplitudes used in refinements are available.[12]

Preparation of $[RhCl(H)(DPM)_2][BPh_4]$. $RhCl_3·3H_2O$ (0.5 g, 1.9 mmol) was refluxed for 3 h in 100 mL of ethanol, which had been refluxed under CO for 0.5 h. This was followed by the addition of 1.46 g (3.8 mmol) of bis(diphenylphosphino)methane (DPM) in 15 mL of benzene and the reflux continued for 10 min. The compound was precipitated by addition of 0.8 g (2.5 mmol) of $NaB(C_6H_5)_4$ and recrystallized from acetone to yield yellow prisms. Elemental analysis and spectral data were essentially identical with those of the crystals initially obtained, one of whose structure is reported (vide infra).

Description of Structure

The unit cell of $[RhCl(H)(DPM)_2][BPh_4]$, shown in Figure 1, contains discrete, well-separated anions and cations. Figure 2 presents a perspective view of the cation including the numbering scheme (phenyl hydrogen atoms have the same number as their attached carbon atom). The inner-coordination sphere of the cation is shown in Figure 3 along with some relevant bond lengths and angles.

The tetraphenylborate anion is not unusual, having a slightly distorted tetrahedral configuration about the boron atom. The B–C distances, shown in Table IV (average 1.69 (2) Å), agree with one another and with other determinations,[13] and the C–B–C angles, shown in Table V, are all close to the expected tetrahedral values.

In the $[RhCl(H)(DPM)_2]^+$ cation the coordination about the Rh(III) center is best described as a slightly distorted quasi-octahedral geometry. The hydrido and chloro ligands are mutually trans in the axial positions and the four equatorial sites are occupied by the phosphorus atoms of the two chelating bis(diphenylphosphino)methane (DPM) ligands. The distortions from the quasi-octahedral geometry in the equatorial plane result from the steric restrictions imposed by the acute DPM bite angle. Thus the intraligand P–Rh–P angles (average 72.45 (7)°) are considerably less than the interligand

Table II. Positional and Thermal Parameters for the Nongroup Atoms of $[RhCl(H)(DPM)_2][BPh_4]$

atom	x^a	*y*	*z*	$U_{11}{}^b$	U_{22}	U_{33}	U_{12}	U_{13}	U_{23}
Rh	0.27510 (2)	0.23489 (3)	−0.08645 (2)	3.58 (3)	5.73 (3)	5.55 (3)	0.04 (2)	0.64 (2)	0.32 (3)
P(1)	0.22634 (8)	0.1105 (1)	−0.05414 (8)	3.70 (7)	5.8 (1)	5.8 (1)	0.15 (7)	0.80 (7)	0.15 (8)
P(2)	0.35601 (8)	0.1865 (1)	0.00614 (8)	3.86 (8)	6.1 (1)	5.03 (9)	0.33 (7)	0.66 (7)	−0.26 (8)
P(3)	0.19008 (9)	0.2889 (1)	−0.1751 (1)	4.28 (9)	7.6 (1)	7.5 (1)	−0.23 (9)	0.08 (9)	2.2 (1)
P(4)	0.31676 (9)	0.3695 (1)	−0.11127 (9)	4.27 (9)	5.9 (1)	7.2 (1)	−0.07 (8)	1.51 (9)	0.49 (9)
Cl	0.3394 (1)	0.1482 (1)	−0.14639 (9)	7.4 (1)	8.9 (1)	7.6 (1)	−0.9 (1)	3.3 (1)	−1.2 (1)
C(1)	0.3097 (3)	0.0817 (5)	0.0071 (3)	4.2 (3)	6.2 (4)	6.0 (4)	0.2 (3)	0.4 (3)	0.4 (3)
C(2)	0.2482 (3)	0.3777 (5)	−0.1879 (4)	4.2 (3)	7.8 (5)	7.2 (5)	0.1 (3)	0.8 (3)	1.7 (4)
C(51)	0.1573 (4)	0.2274 (6)	−0.2471 (4)	6.7 (5)	9.8 (6)	5.9 (5)	−2.4 (4)	−1.1 (4)	2.2 (5)
C(52)	0.1668 (5)	0.1387 (7)	−0.2485 (4)	12.3 (8)	8.6 (7)	7.5 (6)	−3.8 (6)	−1.4 (5)	1.7 (5)
C(53)	0.1399 (7)	0.0912 (8)	−0.3036 (5)	19 (1)	11.2 (9)	8.4 (7)	−5.9 (9)	−1.7 (8)	0.2 (7)
C(54)	0.106 (1)	0.135 (1)	−0.3567 (6)	26 (2)	17 (1)	7.8 (8)	−7 (1)	−6.2 (9)	0.2 (9)
C(55)	0.097 (1)	0.221 (1)	−0.3571 (5)	29 (2)	16 (1)	7.5 (7)	−2 (1)	−7.3 (9)	3.4 (9)
C(56)	0.1241 (8)	0.2689 (8)	−0.3034 (5)	19 (1)	13 (1)	8.4 (8)	−1.4 (9)	−3.0 (8)	2.6 (7)
C(61)	0.1104 (4)	0.3384 (6)	−0.1632 (4)	4.4 (4)	8.9 (6)	9.1 (6)	0.6 (4)	0.7 (4)	4.4 (5)
C(62)	0.1144 (5)	0.4147 (7)	−0.1303 (6)	5.9 (5)	9.3 (7)	18 (1)	2.0 (5)	4.8 (6)	5.2 (8)
C(63)	0.0551 (6)	0.4486 (8)	−0.1154 (7)	8.1 (7)	11.5 (9)	22 (1)	2.6 (6)	6.5 (8)	3.1 (8)
C(64)	−0.0084 (6)	0.402 (1)	−0.1328 (7)	6.7 (7)	17 (1)	18 (1)	4.1 (8)	4.7 (8)	8 (1)
C(65)	−0.0135 (5)	0.328 (1)	−0.1659 (6)	4.8 (5)	19 (1)	11.8 (9)	0.2 (7)	1.2 (6)	7.0 (9)
C(66)	0.0456 (4)	0.2933 (7)	−0.1823 (5)	4.4 (4)	15.2 (9)	10.3 (7)	−0.7 (5)	0.0 (4)	5.3 (7)
B	0.7512 (4)	0.1940 (6)	−0.1624 (4)	5.6 (4)	7.0 (5)	5.8 (5)	0.5 (4)	2.0 (4)	0.2 (4)
H(1)	0.228 (4)	0.279 (5)	−0.051 (3)	6.0 (18)^c					

^{a} Estimated standard deviations in the least significant figure are given in parentheses in this and all subsequent tables. ^{b} The form of the anisotropic thermal ellipsoid is $\exp[-2\pi^2(a^{*2}U_{11}h^2 + b^{*2}U_{22}k^2 + c^{*2}U_{33}l^2 + 2a^*b^*U_{12}hk + 2a^*c^*U_{13}hl + 2b^*c^*U_{23}kl)]$. The quantities given in the table are the thermal coefficients $\times 10^2$. ^{c} Isotropic *B* ($Å^2$).

Table III

Derived Parameters for the Rigid Group Atoms of $[RhCl(H)(DPM)_2][BPh_4]$

atom	*x*	*y*	*z*	*B*, Å^2	atom	*x*	*y*	*z*	*B*, Å^2
C(11)	0.1958 (3)	0.0174 (3)	−0.1057 (2)	3.94 (12)	C(81)	0.4030 (5)	0.3852 (4)	−0.1253 (3)	4.82 (14)
C(12)	0.1230 (3)	−0.0031 (3)	−0.1258 (2)	5.50 (16)	C(82)	0.4533 (5)	0.4418 (4)	−0.0875 (3)	6.80 (20)
C(13)	0.0987 (2)	−0.0712 (3)	−0.1681 (2)	6.62 (19)	C(83)	0.5211 (4)	0.4496 (4)	−0.0961 (3)	8.47 (25)
C(14)	0.1471 (3)	−0.1189 (3)	−0.1904 (2)	6.30 (18)	C(84)	0.5385 (5)	0.4008 (4)	−0.1424 (3)	7.84 (22)
C(15)	0.2199 (3)	−0.0985 (3)	−0.1703 (2)	5.65 (16)	C(85)	0.4881 (5)	0.3442 (4)	−0.1802 (3)	7.09 (21)
C(16)	0.2442 (2)	−0.0303 (3)	−0.1280 (2)	4.59 (14)	C(86)	0.4204 (4)	0.3364 (4)	−0.1716 (3)	6.00 (17)
C(21)	0.1559 (4)	0.1228 (4)	−0.0169 (2)	4.25 (13)	C(91)	0.7063 (3)	0.2832 (3)	−0.2016 (2)	5.10 (15)
C(22)	0.1041 (4)	0.1870 (3)	−0.0396 (3)	5.34 (15)	C(92)	0.6502 (3)	0.2675 (3)	−0.2556 (3)	6.02 (17)
C(23)	0.0422 (3)	0.1884 (3)	−0.0203 (2)	6.37 (18)	C(93)	0.6123 (2)	0.3374 (4)	−0.2897 (2)	7.13 (21)
C(24)	0.0321 (4)	0.1257 (4)	0.0217 (2)	6.79 (20)	C(94)	0.6305 (3)	0.4230 (3)	−0.2699 (2)	7.14 (21)
C(25)	0.0839 (4)	0.0615 (3)	0.0444 (3)	7.51 (22)	C(95)	0.6866 (3)	0.4387 (3)	−0.2158 (3)	7.13 (21)
C(26)	0.1458 (3)	0.0600 (3)	0.0251 (2)	6.40 (18)	C(96)	0.7245 (2)	0.3687 (4)	−0.1817 (2)	5.79 (17)
C(31)	0.3630 (6)	0.2422 (4)	0.0798 (4)	4.71 (14)	C(101)	0.6913 (3)	0.1141 (3)	−0.1664 (2)	5.02 (15)
C(32)	0.3034 (5)	0.2471 (4)	0.1022 (3)	6.97 (21)	C(102)	0.7046 (3)	0.0287 (4)	−0.1818 (2)	6.33 (18)
C(33)	0.3082 (8)	0.2908 (4)	0.1581 (4)	8.14 (24)	C(103)	0.6528 (3)	−0.0358 (3)	−0.1867 (3)	7.52 (22)
C(34)	0.3726 (6)	0.3295 (4)	0.1916 (4)	8.19 (24)	C(104)	0.5876 (3)	−0.0149 (3)	−0.1763 (2)	7.73 (23)
C(35)	0.4322 (5)	0.3246 (4)	0.1692 (3)	8.74 (26)	C(105)	0.5743 (3)	0.0706 (4)	−0.1610 (2)	7.49 (22)
C(36)	0.4274 (8)	0.2809 (4)	0.1133 (4)	6.94 (20)	C(106)	0.6262 (3)	0.1351 (3)	−0.1560 (3)	6.68 (19)
C(41)	0.4480 (2)	0.1618 (3)	0.0099 (2)	4.23 (13)	C(111)	0.7929 (4)	0.2188 (4)	−0.0868 (2)	4.98 (15)
C(42)	0.4842 (3)	0.2160 (3)	−0.0210 (2)	6.51 (19)	C(112)	0.7744 (3)	0.1767 (3)	−0.0382 (4)	5.91 (17)
C(43)	0.5566 (3)	0.2021 (3)	−0.0144 (2)	6.90 (20)	C(113)	0.8113 (4)	0.1958 (3)	0.0238 (3)	6.61 (19)
C(44)	0.5929 (2)	0.1340 (3)	0.0231 (2)	5.94 (17)	C(114)	0.8666 (4)	0.2570 (4)	0.0374 (2)	7.16 (21)
C(45)	0.5568 (3)	0.0797 (3)	0.0540 (2)	5.40 (16)	C(115)	0.8852 (3)	0.2991 (3)	−0.0111 (4)	6.71 (19)
C(46)	0.4843 (3)	0.0936 (3)	0.0474 (2)	4.62 (14)	C(116)	0.8483 (4)	0.2800 (3)	−0.0732 (3)	5.87 (17)
C(71)	0.3053 (3)	0.4629 (3)	−0.0654 (2)	4.94 (14)	C(121)	0.8134 (5)	0.1601 (4)	−0.1962 (5)	5.12 (15)
C(72)	0.2977 (3)	0.4504 (3)	−0.0057 (3)	5.89 (17)	C(122)	0.8025 (3)	0.1675 (4)	−0.2606 (6)	5.79 (17)
C(73)	0.2890 (3)	0.5222 (4)	0.0299 (2)	7.25 (21)	C(123)	0.8534 (8)	0.1348 (4)	−0.2875 (3)	7.17 (21)
C(74)	0.2879 (3)	0.6065 (3)	0.0058 (2)	7.63 (22)	C(124)	0.9152 (5)	0.0947 (4)	−0.2501 (5)	7.76 (23)
C(75)	0.2955 (3)	0.6190 (3)	−0.0538 (3)	7.58 (22)	C(125)	0.9262 (3)	0.0873 (4)	−0.1858 (6)	8.72 (26)
C(76)	0.3042 (3)	0.5472 (4)	−0.0894 (2)	6.55 (19)	C(126)	0.8753 (8)	0.1200 (4)	−0.1588 (3)	6.85 (20)

Rigid Group Parameters

group	X_c[a]	Y_c	Z_c	δ[b]	ϵ	η
Ring 1	0.1714 (2)	−0.0508 (2)	−0.1481 (1)	0.696 (3)	0.167 (4)	1.343 (4)
Ring 2	0.0940 (2)	0.1242 (2)	0.0024 (2)	−0.637 (4)	0.606 (4)	6.263 (4)
Ring 3	0.3678 (2)	0.2858 (2)	0.1357 (2)	4.160 (4)	0.557 (7)	1.151 (7)
Ring 4	0.5205 (2)	0.1479 (2)	0.0165 (1)	2.481 (3)	0.312 (4)	3.336 (3)
Ring 7	0.2966 (2)	0.5347 (3)	−0.0298 (2)	3.080 (4)	1.459 (3)	0.909 (3)
Ring 8	0.4707 (2)	0.3930 (2)	−0.1339 (2)	3.974 (4)	0.521 (5)	3.014 (5)
Ring 9	0.6684 (2)	0.3531 (2)	−0.2357 (2)	−0.032 (4)	2.444 (3)	4.016 (3)
Ring 10	0.6395 (2)	0.0496 (3)	−0.1714 (2)	3.356 (4)	0.406 (3)	5.474 (3)
Ring 11	0.8298 (2)	0.2379 (2)	−0.0247 (2)	3.956 (3)	1.871 (5)	0.310 (5)
Ring 12	0.8643 (2)	0.1274 (2)	−0.2232 (2)	2.058 (4)	1.563 (8)	4.014 (7)

[a] X_c, Y_c, and Z_c are the fractional coordinates of the centroid of the rigid group. [b] The rigid group orientation angles δ, ϵ, and η (radians) are the angles by which the rigid body is rotated with respect to a set of axes *X*, *Y*, and *Z*. The origin is the center of the ring; *X* is parallel to a^*, *Z* is parallel to *c*, and *Y* is parallel to the line defined by the intersection of the plane containing a^* and b^* with the plane containing *b* and *c*.

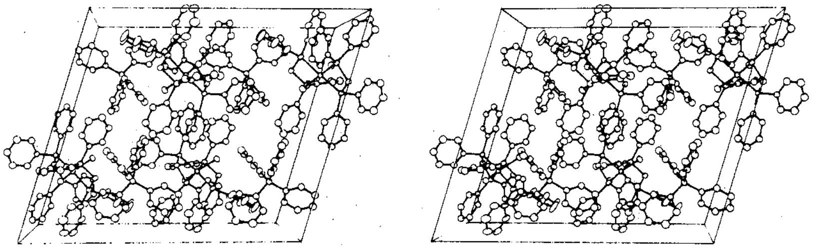

Figure 1. A stereoview of the cell of $[RhCl(H)(DPM)_2][BPh_4]$. The *z* axis is horizontal to the right, the *x* axis runs from bottom to top, and the *y* axis comes out of the page; 20% vibrational ellipsoids are used on all drawings except methylene hydrogens which are drawn artificially small.

values (average 107.29 (7)°). The four phosphorus atoms are essentially coplanar (see Table VI) with the Rh atom displaced 0.1145 (5) Å from this plane, toward the chloro ligand. Likewise the two methylene carbon atoms are displaced from their respective P–Rh–P chelate planes by an average of 0.338 (7) Å, again in the direction of the chloro ligand. The Rh-$(DPM)_2$ framework (including the rhodium atom, the four phosphorus atoms, and the two methylene carbon atoms) is therefore slightly puckered and has a flattened "W" configuration when viewed in the plane of the four phosphorus atoms, looking along the bisector of the P(2)–Rh–P(4) or the P(1)–Rh–P(3) angle (see Figure 2). This puckering is evident from the angles between the two P–Rh–P chelate planes (172.59°) and from the angles between the P–Rh–P and the P–C–P planes (average 16.05°). Although the authors claim that in $[Mo(CO)_4(DPM)]$ the chelate ring is planar,[14] a close inspection of their data reveals that this ring is also puckered somewhat. In contrast, the Fe–DPM framework in [Fe-

Table IV. Selected Distances (Å) in $[RhCl(H)(DPM)_2][BPh_4]$

Bond Distances					
Rh-Cl	2.465 (2)		C(51)-C(52)	1.369 (13)	
Rh-H(1)	1.51 (7)		C(51)-C(56)	1.385 (12)	
Rh-P(1)	2.329 (2)	2.329 (3)[a]	C(52)-C(53)	1.390 (13)	
Rh-P(2)	2.324 (2)		C(53)-C(54)	1.353 (16)	
Rh-P(3)	2.329 (2)		C(54)-C(55)	1.322 (19)	
Rh-P(4)	2.334 (2)		C(55)-C(56)	1.371 (17)	
P(1)-C(1)	1.845 (6)	1.842 (7)	C(61)-C(62)	1.367 (13)	
P(2)-C(1)	1.841 (7)		C(61)-C(66)	1.392 (11)	
P(3)-C(2)	1.841 (7)		C(62)-C(63)	1.392 (13)	
P(4)-C(2)	1.842 (7)		C(63)-C(64)	1.377 (16)	
P(1)-C(11)	1.817 (4)	1.811 (9)	C(64)-C(65)	1.345 (17)	
P(1)-C(21)	1.807 (4)		C(65)-C(66)	1.406 (15)	
P(2)-C(31)	1.818 (4)		B-C(91)	1.714 (9)	1.689 (16)
P(2)-C(41)	1.810 (4)		B-C(101)	1.671 (9)	
P(3)-C(51)	1.809 (9)		B-C(111)	1.689 (9)	
P(3)-C(61)	1.813 (8)		B-C(121)	1.683 (9)	
P(4)-C(71)	1.806 (4)				
P(4)-C(81)	1.811 (4)				
Nonbonded Distances					
P(1)-P(2)	2.750 (2)		H(25)-H(126)	2.28	
P(3)-P(4)	2.755 (2)		H(96)-H(116)	2.14	
P(1)-P(3)	3.751 (3)		C(61)-H(22)	2.68	
P(2)-P(4)	3.751 (3)		C(66)-H(22)	2.67	
Rh-C(1)	3.074 (7)		C(81)-H(42)	2.58	
Rh-C(2)	3.074 (7)				

[a] For averaged quantities the estimated standard deviation is the larger of the estimated standard deviation or the standard deviation of a single observation as calculated from the mean.

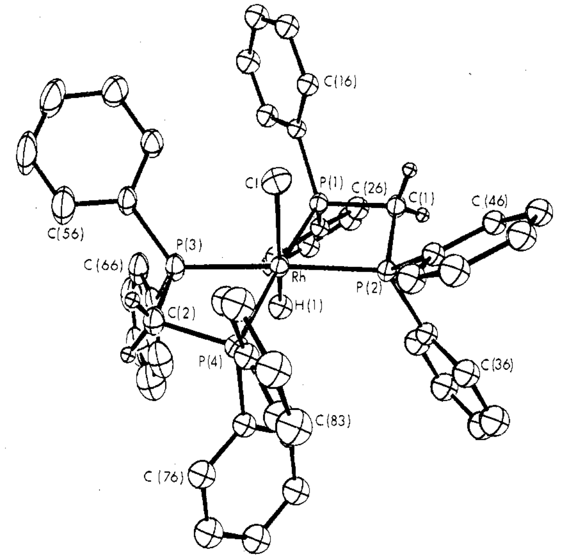

Figure 2. A perspective view of the $[RhCl(H)(DPM)_2]^+$ cation showing the numbering scheme. The numbering on the phenyl carbon atoms starts at the carbon bonded to phosphorus and increases sequentially around the ring.

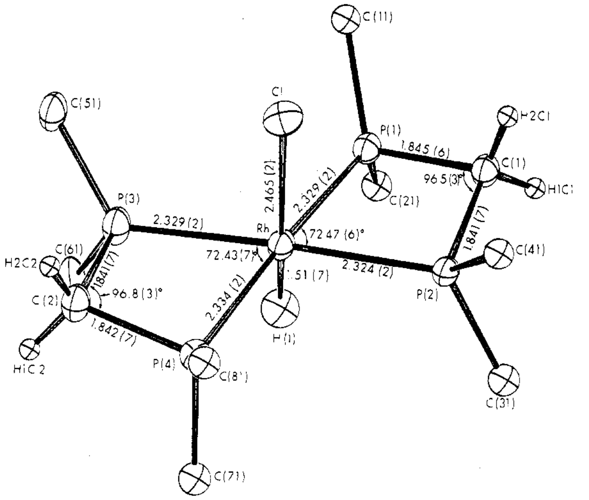

Figure 3. The inner-coordination sphere of the $[RhCl(H)(DPM)_2]^+$ cation showing some relevant bond lengths and angles. Only the first carbon atom of each phenyl ring is shown.

$(CO)_3(DPM)]$ is essentially planar.[15] Thus the present structure has its DPM groups intermediate between the planar configuration observed in $[Fe(CO)_3(DPM)]$ and the folded configuration observed when the DPM ligand is bridging[1,2,16-19] (here the methylene carbon atoms are ca. 0.65–0.75 Å out of the M–P–P–M planes). It is expected that the folding of the methylene groups reflects an attempt to minimize steric interactions and in the present complex allows the phenyl rings to avoid the bulkier chloro ligand and move closer instead to the less sterically encumbered hydrido ligand.

The Rh–P bond distances (average 2.329 (3) Å) are somewhat shorter than is usually observed for Rh(III) complexes when phosphine ligands are mutually trans (2.368 (3)–2.415 (4) Å)[20-22] but compare well with those reported for other rhodium–DPM complexes (2.305 (4)–2.333 (8) Å).[1-3] The P–C distances (both methylene and phenyl) are quite typical for DPM ligands and the intraligand P–Rh–P angles (average 72.45 (7)°) fall within the range previously reported for chelating DPM ligands (73.5 (1)–67.3 (1)°).[14,15,23] The Rh–P–C(methylene) and P–C–P angles (average 94.3 (2) and 96.6 (3)°, respectively) are significantly distorted from their expected tetrahedral values owing to the strain imposed by the four-membered ring. In contrast, values near 109° are observed when DPM ligands bridge two metals.[1,2,16-19]

The phenyl rings are arranged around the periphery of the $Rh(DPM)_2$ frame such that four are above the chelate planes and four are below. Within each of these groups of four phenyl rings, all adjacent rings are essentially eclipsed as can be seen in Figure 2 and as is evident from the phenyl–P–P–phenyl torsion angles (0.1 (4)–6.1 (3)°), shown in Table V. This, however, does not lead to any unusually short contacts between the rings. Phenyl rings 5 and 6, which were refined as individual anisotropic atoms, are of approximate D_{6h} symmetry, as expected; both are essentially planar (see Table VI), their C–C–C bond angles are close to 120° (Table V), and their

Table V. Selected Angles (deg) in $[RhCl(H)(DPM)_2][BPh_4]$

Bond Angles

Cl-Rh-H(1)	172 (3)	Rh-P(3)-C(51)	123.4 (3)	P(3)-C(51)-C(56)	121.2 (9)
Cl-Rh-P(1)	92.66 (7)	Rh-P(3)-C(61)	116.9 (3)	P(3)-R(61)-C(62)	121.0 (7)
Cl-Rh-P(2)	89.43 (7)	Rh-P(4)-C(71)	116.9 (2)	P(3)-C(61)-C(66)	119.2 (9)
Cl-Rh-P(3)	94.53 (8)	Rh-P(4)-C(81)	124.1 (2)	P(4)-C(71)-C(72)	119.8 (3)
Cl-Rh-P(4)	94.50 (7)	C(1)-P(1)-C(11)	109.7 (3)	P(4)-C(71)-C(76)	120.2 (3)
H(1)-Rh-P(1)	81 (3)	C(1)-P(1)-C(21)	107.9 (3)	P(4)-C(81)-C(82)	120.2 (3)
H(1)-Rh-P(2)	92 (3)	C(1)-P(2)-C(31)	107.7 (3)	P(4)-C(81)-C(86)	119.7 (3)
H(1)-Rh-P(3)	84 (3)	C(1)-P(2)-C(41)	107.4 (3)	C(51)-C(52)-C(53)	121.1 (9)
H(1)-Rh-P(4)	92 (3)	C(2)-P(3)-C(51)	108.6 (4)	C(52)-C(53)-C(54)	118 (1)
P(1)-Rh-P(2)	72.47 (6)	C(2)-P(3)-C(61)	107.9 (4)	C(53)-C(54)-C(55)	122 (1)
P(1)-Rh-P(3)	107.29 (6)	C(2)-P(4)-C(71)	107.3 (3)	C(54)-C(55)-C(56)	120 (1)
P(1)-Rh-P(4)	172.84 (7)	C(2)-P(4)-C(81)	106.9 (3)	C(55)-C(56)-C(51)	120 (1)
P(2)-Rh-P(3)	176.04 (7)	C(11)-P(1)-C(21)	102.6 (2)	C(56)-C(51)-C(52)	117.6 (9)
P(2)-Rh-P(4)	107.29 (7)	C(31)-P(2)-C(41)	104.0 (2)	C(61)-C(62)-C(63)	121 (1)
P(3)-Rh-P(4)	72.43 (7)	C(51)-P(3)-C(61)	104.4 (4)	C(62)-C(63)-C(64)	119 (1)
P(1)-C(1)-P(2)	96.5 (3)	C(71)-P(4)-C(81)	105.5 (3)	C(63)-C(64)-C(65)	120 (1)
P(3)-C(2)-P(4)	96.8 (3)	P(1)-C(11)-C(12)	119.7 (3)	C(64)-C(65)-C(66)	121 (1)
Rh-P(1)-C(1)	94.2 (2)	P(1)-C(11)-C(16)	120.2 (3)	C(65)-C(66)-C(61)	118 (1)
Rh-P(2)-C(1)	94.5 (2)	P(1)-C(21)-C(22)	118.2 (3)	C(66)-C(61)-C(62)	119.4 (9)
Rh-P(3)-C(2)	94.2 (2)	P(1)-C(21)-C(26)	120.7 (3)	C(91)-B-C(101)	107.9 (5)
Rh-P(4)-C(2)	94.1 (2)	P(2)-C(31)-C(32)	119.8 (3)	C(91)-B-C(111)	110.9 (6)
Rh-P(1)-C(11)	122.0 (2)	P(2)-C(31)-C(36)	120.2 (3)	C(91)-B-C(121)	110.1 (5)
Rh-P(1)-C(21)	119.3 (2)	P(2)-C(41)-C(42)	119.3 (3)	C(101)-B-C(111)	110.1 (6)
Rh-P(2)-C(31)	120.5 (2)	P(2)-C(41)-C(46)	120.5 (3)	C(101-B-C(121)	109.5 (6)
Rh-P(2)-C(41)	121.0 (2)	P(3)-C(51)-C(52)	121.2 (6)	C(111)-B-C(121)	108.4 (5)

Torsion Angles

P(1)-P(2)-P(4)-P(3)	2.72 (8)	C(21)-P(1)-P(2)-C(31)	−1.1 (3)	C(41)-P(2)-P(4)-C(71)	113.4 (3)
C(1)-P(1)-P(3)-C(2)	4.3 (5)	C(21)-P(1)-P(2)-C(41)	−151.1 (3)	C(41)-P(2)-P(4)-C(81)	4.1 (3)
C(1)-P(2)-P(4)-C(2)	4.4 (4)	C(21)-P(1)-P(3)-C(51)	107.9 (3)	C(51)-P(3)-P(4)-C(71)	−150.4 (5)
C(11)-P(1)-P(2)-C(31)	150.2 (3)	C(21)-P(1)-P(3)-C(61)	0.5 (4)	C(51)-P(3)-P(4)-C(81)	−1.6 (5)
C(11)-P(1)-P(2)-C(41)	0.1 (4)	C(31)-P(2)-P(4)-C(71)	6.1 (3)	C(61)-P(3)-P(4)-C(71)	0.3 (4)
C(11)-P(1)-P(3)-C(51)	2.4 (3)	C(31)-P(2)-P(4)-C(81)	−103.2 (3)	C(61)-P(3)-P(4)-C(81)	149.2 (4)
C(11)-P(1)-P(3)-C(61)	−105.0 (3)				

Table VI

Least-Squares Plane Calculations[a]

plane no.	equation	plane no.	equation
1	$0.6281X - 0.5738Y - 0.5256Z - 2.6272 = 0.0$	5	$0.6457X - 0.5211Y - 0.5581Z - 2.8664 = 0.0$
2	$0.6652X - 0.4649Y - 0.5842Z - 3.3457 = 0.0$	6	$0.9728X + 0.1221Y - 0.1969Z - 6.0087 = 0.0$
3	$0.6166X - 0.3583Y - 0.7010Z - 3.1385 = 0.0$	7	$-0.0159X + 0.5160Y - 0.8564Z - 5.5991 = 0.0$
4	$0.6479X - 0.6586Y - 0.3827Z - 1.6555 = 0.0$		

Deviations from the Planes (Å)

	plane no.						
atom	1	2	3	4	5	6	7
Rh	0.0	0.0			0.1145 (5)[b]		
P(1)	0.0		0.0		−0.029 (2)		
P(2)	0.0		0.0		0.029 (2)		
P(3)		0.0		0.0	−0.033 (2)		
P(4)		0.0		0.0	0.040 (2)		
C(1)	0.338 (7)[b]		0.0		0.265 (7)[b]		
C(2)		0.339 (7)[b]		0.0	0.272 (7)[b]		
C(51)						−0.015 (9)	
C(52)						0.015 (11)	
C(53)						−0.005 (15)	
C(54)						−0.008 (19)	
C(55)						−0.007 (20)	
C(56)						0.024 (15)	
C(61)							−0.005 (9)
C(62)							−0.001 (12)
C(63)							0.012 (13)
C(64)							−0.015 (15)
C(65)							0.000 (13)
C(66)							0.007 (10)

Dihedral Angles between Planes

plane A	plane B	angle, deg
1	2	7.41
1	3	15.99
2	4	16.10

[a] *X*, *Y*, and *Z* are the orthogonal coordinates (Å) with *X* along the *a* axis, *Y* in the (*a*-*b*) plane, and *Z* along the *c** axis. [b] Not included in least-squares plane calculation.

bond lengths, although slightly contracted as a result of thermal motion, are not unreasonable (Table IV).

The Rh–H distance of 1.51 (7) Å falls within the range of 1.5–1.7 Å normally observed for second-row transition-metal hydrides.[24] This hydrido ligand, which is trans to the chloro ligand (the Cl–Rh–H angle is 172 (3)°), shows the expected high trans influence resulting in a long Rh–Cl bond distance of 2.465 (2) Å. This distance is significantly longer than the Rh–Cl distance of 2.387 (4) Å in $RhCl(H)(SiMe_3)(PPh_3)_2$ where the hydrido and chloro ligands are again mutually trans[25] and is also longer than Rh(III)–Cl distances when two chloro ligands are mutually trans (2.29 (1)–2.365 (6) Å).[20,22,26] In fact, on the basis of a comparison of Rh(III)–Cl distances, the trans influence exerted by the present hydride is comparable to that exerted by σ-bound alkyl groups and carbenes.[27]

Discussion

It is well-known that the DPM ligand can function as either a bridging[1–4,16–19] or chelating[14,15,23] bidentate ligand in transition-metal complexes. With rhodium, numerous examples of bridging DPM ligands are known; however, this is believed to be the first example in which the DPM ligand chelates a rhodium center; it is certainly the first structurally characterized example. We find this somewhat startling since several examples of chelating DPM systems with ruthenium[28] and iron[15] are known. Furthermore, the DPM ligand presents an interesting contrast to the bis(diphenylphosphino)ethane (DPPE) ligand which has a known propensity for chelating in rhodium chemistry[29,30] but which has never been observed to bridge two rhodium centers while bonding via the phosphorus atoms (an unusual bridging coordination has been observed in $[Rh_2(Ph_2P(CH_2)_2PPh_2)_2]^{2+}$ in which each Rh atom is bonded to the two P atoms of one DPPE ligand and to a phenyl ring of the DPPE ligand on the second Rh atom).[31] Since rhodium complexes in which the DPM ligands are either bridging or chelating have now been characterized, it is of obvious interest to obtain the elusive species having the DPPE ligand bridging two rhodium centers. Work is now underway in our laboratory in pursuit of this goal.

Having established that the complex of interest was the DPM-chelated, hydridorhodium complex, it was of obvious interest to establish the origin of this unexpected product. It did not seem reasonable to us that this species resulted from the reactions involving SO_2. Rather, it seemed more likely that it arose in the initial preparation of the "A-frame" complex, **1**, and was merely present in subsequent reactions as an impurity. The species present when $RhCl_3{\cdot}3H_2O$ is refluxed under CO in ethanol/water is the anion $[RhCl_2(CO)_2]^-$.[32] Reaction of this anion with DPM then yields complex **1**. However, it had been noted that with a slight excess of DPM, complex **1** was contaminated with other, unidentified species. Since an excess of DPM would tend to favor our chelated species instead of the bridged species **1**, we repeated the above reaction with a deliberate DPM:Rh molar ratio of 2:1. The DPM-chelated hydrido species was obtained in about 85% yield and was identified by a comparison of its ^1H and ^{31}P NMR spectra, its infrared spectrum, and its elemental analysis with those of the structurally characterized product. We postulate, therefore that the hydrido species was present as an impurity in the solution of complex **1** and precipitated owing to changes in solubility resulting possibly from saturation of the acetone solution with SO_2 or concentration of the solution resulting from solvent evaporation. The source of the hydrido ligand is then readily explained as resulting from the H_2O/ethanol mixture.

In conclusion, the reaction of the $[RhCl_2(CO)_2]^-$ anion with DPM yields two products depending on the DPM:Rh molar ratio. With a 1:1 ratio the expected binuclear species $[Rh_2(CO)_2(\mu\text{-}Cl)(DPM)_2]^+$ is obtained,[1] whereas utilizing an excess of DPM the molecular hydrido species $[RhCl(H)(DPM)_2]^+$, having chelating DPM ligands, is obtained.

Acknowledgment. The authors thank The University of Alberta and the Natural Sciences and Engineering Research Council Canada for financial support and NSERC for a scholarship to S.K.D.

Registry No. **1**, 67202-35-1; $[RhCl(H)(DPM)_2][BPh_4]$, 69501-92-4.

Supplementary Material Available: Tables VII and VIII, showing the idealized hydrogen parameters and the root-mean-square amplitudes of vibration of the individual atoms, respectively, and a listing of the observed and calculated structure amplitudes (34 pages). Ordering information is given on any current masthead page.

References and Notes

(1) M. Cowie, J. T. Mague, and A. R. Sanger, *J. Am. Chem. Soc.*, **100**, 3628 (1978), and references therein.
(2) M. Cowie, *Inorg. Chem.*, **18**, 286 (1979).
(3) M. Cowie, S. K. Dwight, and A. R. Sanger, *Inorg. Chim. Acta*, **31**, L407 (1978).
(4) M. Cowie and S. K. Dwight, to be submitted for publication.
(5) The great discrepancy between the calculated and observed analyses for chlorine results from the method used by our departmental analytical services laboratory (Schöniger's method) which is highly susceptible to interference by rhodium–phosphorus compounds. The observed value was obviously misleading to us in our early stages of formulation of the complex since it indicated that no chlorine was present.
(6) R. J. Doedens and J. A. Ibers, *Inorg. Chem.*, **6**, 204 (1967).
(7) Besides local programs and some kindly supplied by J. A. Ibers and D. J. Hodgson, the following were used in solution and refinement of the structure: FORDAP, the Fourier summation program by A. Zalkin; GONO2, absorption and extinction program by W. C. Hamilton; SFLS5, structure factor and least-squares refinement by C. J. Prewitt; ORFFE, for calculating bond lengths, angles, and associated standard deviations by W. Busing and H. A. Levy; ORTEP, plotting program by C. K. Johnson.
(8) D. T. Cromer and J. T. Waber, "International Tables for X-Ray Crystallography", Vol. IV, Kynoch Press, Birmingham, England, 1974, Table 2.2A.
(9) R. F. Stewart, E. R. Davidson, and W. T. Simpson, *J. Chem. Phys.*, **42**, 3175 (1965).
(10) D. T. Cromer, *Acta Crystallogr.*, **18**, 17 (1965).
(11) $R = \sum||F_o| - |F_c||/\sum|F_o|$; $R_w = [\sum w(|F_o| - |F_c|)^2/\sum wF_o^2]^{1/2}$.
(12) Supplementary material.
(13) P. Dapporto, S. Midollini, and L. Sacconi, *Inorg. Chem.*, **14**, 1643 (1975); E. J. Laskowski, D. M. Duggan, and D. N. Hendrickson, *ibid.*, **14**, 2449 (1975); C. Mealli, S. Midollini, and L. Sacconi, *ibid.*, **14**, 2513 (1975); W. K. Dean, R. S. Charles, and D. G. Van Derveer, *ibid.*, **16**, 3328 (1977), and references therein; E. J. Laskowski and D. N. Hendrickson, *ibid.*, **17**, 457 (1978).
(14) K. K. Cheung, T. F. Lai, and K. S. Mok, *J. Chem. Soc. A*, 1644 (1971).
(15) F. A. Cotton, K. I. Hardcastle, and G. A. Rusholme, *J. Coord. Chem.*, **2**, 217 (1973).
(16) F. H. Carré, F. A. Cotton, and B. A. Frenz, *Inorg. Chem.*, **15**, 380 (1976).
(17) F. A. Cotton and J. M. Troup, *J. Am. Chem. Soc.*, **96**, 4422 (1974).
(18) A. Camus, G. Nardin, and L. Randaccio, *Inorg. Chim. Acta*, **12**, 23 (1975).
(19) G. Nardin, L. Randaccio, and E. Zangrando, *J. Chem. Soc., Dalton Trans.*, 2566 (1975).
(20) F. H. Allen, G. Chang, K. K. Cheung, T. F. Lai, and L. M. Lee, *J. Chem. Soc., Chem. Commun.*, 1297 (1970).
(21) B. Cetinkaya, M. F. Lappert, G. M. McLaughlin, and K. Turner, *J. Chem. Soc., Dalton Trans.*, 1591 (1974).
(22) A. C. Skapski and F. A. Stephens, *J. Chem. Soc., Dalton Trans.*, 1789 (1975).
(23) W. L. Steffen and G. J. Palenik, *Inorg. Chem.*, **15**, 2432 (1976).
(24) B. A. Frenz and J. A. Ibers, "Transition Metal Hydrides", E. L. Muetterties, Ed., Marcel Dekker, New York, N.Y., 1971, Chapter 3.
(25) L. Monojlovic-Muir, K. W. Muir, and J. A. Ibers, *Inorg. Chem.*, **9**, 440 (1970).
(26) J. A. Evans, D. R. Russell, A. Bright, and B. L. Shaw, *Chem. Commun.*, 841 (1971).
(27) M. Cowie and J. A. Ibers, *Inorg. Chem.*, **15**, 522 (1976), and references therein.
(28) J. Chatt and R. G. Hayter, *J. Chem. Soc.*, 896 (1961); 2605 (1961); 6017 (1963).
(29) A. R. Sanger, *J. Chem. Soc., Dalton Trans.*, 1971 (1977), and references therein.
(30) A. Sacco and R. Ugo, *J. Chem. Soc.*, 3274 (1964).
(31) J. Halpern, D. P. Riley, A. S. C. Chan, and J. J. Pluth, *J. Am. Chem. Soc.*, **99**, 8055 (1977).
(32) J. T. Mague and J. P. Mitchener, *Inorg. Chem.*, **8**, 119 (1969).